Time-calibrated genomic evolution of a monomorphic bacterium during its establishment as an endemic crop pathogen

Running title: Genomic evolution of an emergent pathogenic bacterium

Damien Richard[a,b,c,#]

Olivier Pruvost[a]

François Balloux[d]

Claudine Boyer[a]

Adrien Rieux[a]

Pierre Lefeuvre[a]

[a] Cirad, UMR PVBMT, F-97410 St Pierre, Réunion, France.
[b] ANSES, Plant Health Laboratory, F-97410 St Pierre, Réunion, France.
[c] Université de la Réunion, UMR PVBMT, F-97490 St Denis, Réunion, France.
[d] UCL Genetics Institute, University College London, London WC1E 6BT, UK.
[#] Corresponding author: Damien Richard, richarddamienfr@gmail.com

Competing interests

The authors declare that they have no competing interests.

Keywords

Genomic evolution; Dated phylogeny; Citrus canker; Gene turnover rate; SNP substitution rate

Abstract

The reconstruction of the evolutionary histories of pathogen populations in space and time often improves our understanding of their epidemiology. However, analyses are usually restricted to the non-recombining genomic regions and, thus, fail to inform on the dynamics of the accessory genome. Yet, horizontal gene transfer is of striking importance to the evolution of bacteria as it can redistribute phenotypically important genes. For bacterial pathogens, those include resistance to antimicrobial compounds and virulence factors. Although understanding the gene turnover in genomes at microevolutionary scales is key to apprehend the pace of this evolutionary process, few studies are available. Here we addressed this question for the epidemic lineage of *Xanthomonas citri* pv. *citri*, a bacterial plant pathogen of major agricultural importance worldwide. Relying on a dense geographic sampling spanning 39 years of evolution, we estimated both the dynamics of Single Nucleotide Polymorphism accumulation and the gene content turnover. We showed extensive gene content variation among the lineage even at the smallest phylogenetic and geographic scales. Gene turnover rate exceeded SNP mutation rates by three orders of magnitude. Accessory genes were preferentially plasmid-encoded, but we evidenced a highly plastic chromosomal region hosting ecologically important genes such as transcription activator-like effectors. We argue that turnover of accessory genes provides a potent evolutionary force in monomorphic bacteria, and exemplify this statement retracing the history of a mobile element conferring resistance to copper compounds widely used for the management of plant bacterial pathogens.

Introduction

Recently, the retrospective analysis of time and geographically informed genomic datasets has gained in popularity for reconstructing the evolutionary history of pathogens (1). It can shed light on the pathogens' origin and transmission pathways, as well as on the evolution of key phenotypes (2, 3). In addition to time calibrating the pathogens' evolution, genomic datasets can be used to quantify the importance of gene content variation relative to nucleotide substitution. Understanding bacterial core-genome kinship is important per se. However, the concomitant reconstruction of ancestral gene content in a combined approach has recently shown promise for deciphering transmission, geographical expansion and host specificity for the study of plant pathogenic bacteria (4-6). This is particularly relevant for bacterial lineages that display low SNP substitution rates (referred to as monomorphic (7)) and/or that have an open pan-genome. Gain and loss of accessory genes, primarily achieved through plasmid or bacteriophage acquisition (7-9) plays an important role in bacterial genomic evolution (10). Indeed, multiple genome-wide studies evidenced large gene content variation between otherwise closely related bacteria (10-14). Studies to determine the rate of gene content variations are still scarce (15-19). Yet, horizontally acquired DNA sometimes greatly improves the fitness of a bacterial lineage, by providing novel functions, such as enhanced in-host multiplication, the ability to colonize a new ecological niche or antimicrobial resistance (20-22). In particular, the evolution of the gene content through plasmid acquisition is an efficient way to acquire the full set of genes necessary for a given function in a single step. Indeed, several pathogens have emerged following the acquisition of a single plasmid (23-25).

Xanthomonas citri pv. *citri* (*Xcc*) is a monomorphic bacterium, whose genome was reported to display variations through differences in genomic island composition (26) or plasmid content (27, 28). *Xcc* is the causal agent of the Asiatic citrus canker, an economically important disease that threatens citrus industries in most areas of production. Although the pathogen is disseminated over short distances by wind and rain and the use of contaminated tools, its worldwide diffusion is primarily due to the movement of contaminated plant material (29). Population genomic data can unravel the long distance movements of *Xcc*. For example, in the South West Indian Ocean (SWIO) area, the pathogen has been described in Réunion (30), Rodrigues (31), Mauritius (32) Comoros (33) and Seychelles (34). However, historical reports are scarce, which makes it difficult to determine the time frame and numbers involved in *Xcc* introduction and diffusion. Asiatic citrus canker control largely relies on the removal of contaminated trees or integrated management, involving repeated applications of copper-based

pesticides (35). In Réunion over the last decade, copper resistance has emerged with the integration of a mobile heavy metal resistance plasmid (pCu^R) (27). A first microsatellite-based analysis suggested that local *Xcc* strains had acquired resistance from an unknown source and that foreign *Xcc* strains had not been introduced. The emergence of this new adaptive phenotype in an area of disease endemicity provides an interesting opportunity to compare long- and short-term evolution and assess the importance of gene turnover in the evolution of *Xcc*. To this end, we conducted whole genome sequencing for 221 strains collected on the SWIO islands. Importantly, the 39-year timespan for the sampling dates made it possible to estimate the evolutionary rate of *Xcc*. From this dataset, we determined the gene and nucleotide substitution rates in order to quantify their respective effect on genome evolution. Besides time calibrating and quantifying *Xcc* evolution, we put forward a hypothesis on the long-term history of *Xcc* in the SWIO region, going back to its first probable introduction in the 19th century.

Results

Global phylogeny

The analysis of 284 strains representing worldwide *Xcc* diversity with a particular emphasis on the SWIO islands (Figure 1) revealed 7 005 high confidence SNPs. The phylogenetic reconstruction obtained from this set displayed a strong geographic structure (Supplementary Figure S1). Whilst some subclades comprising worldwide strains remained unresolved, all 210 strains sampled from the SWIO region formed a well-resolved monophyletic clade. The 20 strains from the northern Indian Ocean (Maldives and Seychelles) formed four subclades, which were genetically distinct from the SWIO strains and more closely related to strains from the Indian sub-continent. Consistent with previous data (20), copper-resistant (Cu^R) *Xcc* from Martinique (French West Indies) were closely related to most Cu^R strains isolated from Réunion.

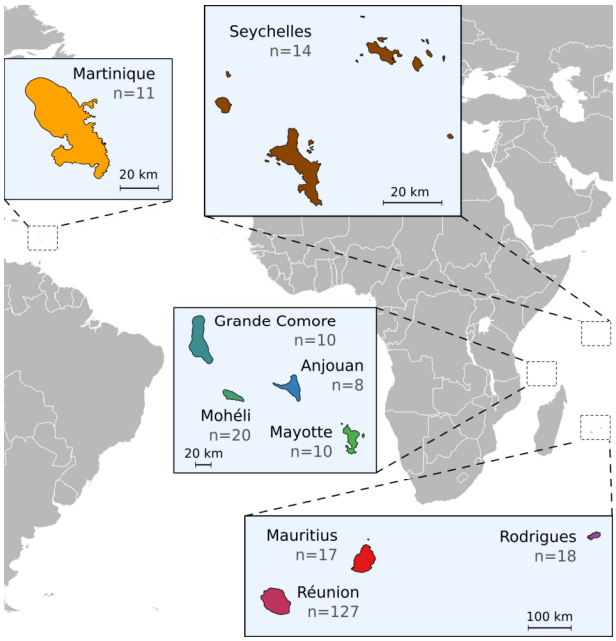

Figure 1. Location of the South West Indian Ocean islands where the majority of the strains studied were sampled. Number of strains per location is indicated in parentheses.

Genetic structuring between and within islands

Within the SWIO clade, strains sampled from the same island or archipelago tend to form discrete subclades (Figure 2). All 48 strains from the Comoros Archipelago were in the SNP subclade number 2, with no clear genetic delineation between islands (Figure 2). Twelve Mauritian strains were in the well-defined subclade 4, while the five remaining Mauritian strains were scattered in the SWIO clade

(Figure 2). Lastly, strains sampled in Réunion were genetically diverse and belonged to several distinct SWIO subclades. Within Réunion, extensive strain sampling was conducted in 13 groves and one nursery (four to 17 strains per site). No obvious spatial structure was apparent at this scale and all but one of the citrus groves hosted strains from multiple Réunion subclades (Supplementary Figure S1B).

Temporal signal and time calibration

Although there was no significant temporal signal for the global phylogeny, the regression between the root-to-tip distance and node age was significant (*p*-value 2.3×10^{-4} and R^2 0.06) at the root of the SWIO clade with a slope of 3.2×10^{-5} (Supplementary Figure S2B). The temporal signal for the SWIO clade was further confirmed by a date-randomization test (Supplementary Figure S2A).

A time-calibrated analysis was conducted using the BEAST framework (36) on the 221 strains of the SWIO clade, using an exponential growth tree model and an uncorrelated lognormal relaxed clock (estimated standard deviation: 0.26 (95% HPD 0.18-0.34)). Overall, the Maximum Likelihood and the Bayesian trees had a similar topology (Supplementary Figure S3). The SWIO tree root age was established at around 1818 (95% HPD: 1762-1868, Table 1), with an estimated substitution rate of 8.4×10^{-8} substitutions per site per year (95% HPD: 6.9×10^{-8}-1.0×10^{-7}). This corresponds to 0.43 SNP substitutions per genome per year (95% HPD: 0.35-0.51).

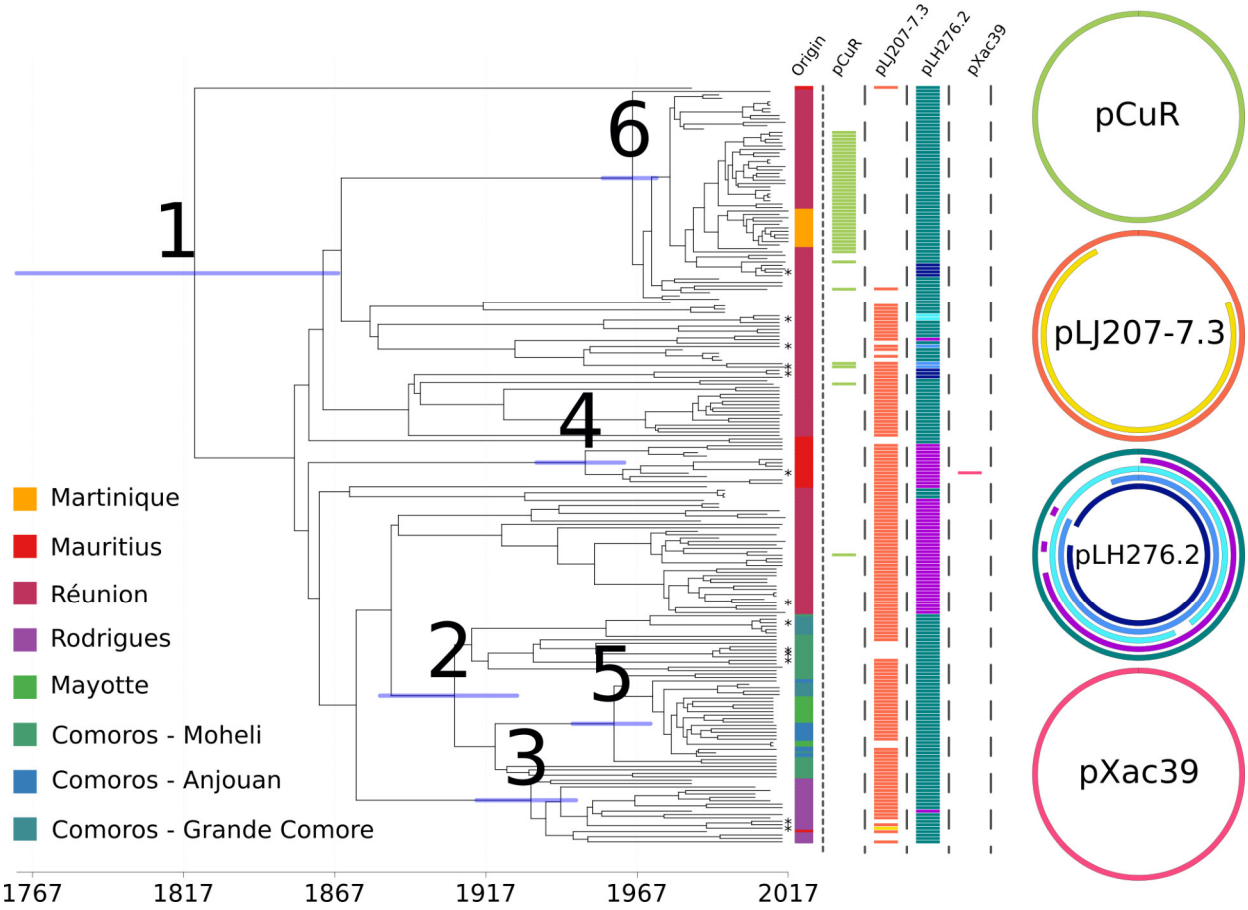

Figure 2. A dated phylogeny of the SWIO clade of *Xanthomonas citri* pv. *citri*. X-axis under the phylogenetic tree represents the timescale in years (AD). Node bars represent 95% highest posterior density (HPD) for node ages estimated with tip-calibration. Tips are coloured according to sampling location. Coloured boxes indicate the plasmid content of each strain. The colour code for the boxes matches the colours for the represented circular plasmids and corresponds to observed plasmid alleles. Node numbers correspond to those in Table 1. Tip labels with asterisks indicate strains for which long-read sequencing was also performed.

Table 1. Inferred dates of MRCA and substitution rates of the SWIO clade along with those of five clades of interest.

Node number	Inferred node date	Date 95% confidence interval	No. of strains	No. of variable genes	No. of variable SNPs	Subst. rate SNP	No. of core-genome genes	No. of pan-genome genes
1	1818	1762-1868	221	699	3403	8.8E-8	4347	5046
2	1906	1882-1927	48	205	812	8.8E-8	4546	4751
3	1931	1914-1947	19	222	363	8.8E-8	4531	4753
4	1949	1934-1963	12	143	134	8.5E-8	4611	4754
5	1959	1946-1971	27	147	288	8.3E-8	4593	4740
6	1965	1956-1973	62	358	318	8.1E-8	4599	4957

Accessory genome content

In order to test our ability to detect the gene content of *Xcc* strains properly, two strains were sequenced in triplicate before the application of the gene content inference pipeline. Gene content was similar between all replicates for one of the strains, while six genes were variably detected for the other strain, with a maximum difference of four non-syntenic genes between replicates. A very low fraction of unique genes can be erroneously detected in unique individuals. However, it is likely that events involving the gain or loss of numerous genes or the display of a phylogenetic signal (i.e. when the same event is revealed in closely related individuals) are genuine.

After *de novo* genome assembly, gene detection and gene clustering of the 221 SWIO strains, a pan-genome size of 5 046 genes was identified. The core genome comprised 4 347 genes (i.e. detected in all strains), while the accessory genome comprised 699 genes (i.e. absent from at least one strain). Of these accessory genes, 336 were assigned to the chromosome, 339 to plasmids and 24 remained unassigned (Figure 3). Most of the accessory genes (70%) did not match any known Cluster of Orthologous Group (COG); 4% matched replication, recombination and repair functions; 3% inorganic ion transport and other COG categories each comprised fewer than 3% of the gene clusters. As shown by the analysis of replicate control, our gene detection pipeline may have limitations associated with the detection of unique genes that have been gained or lost in single strains. Fourteen out of 699 genes displayed such characteristics. We then used a Bayesian reconstruction of the ancestral states in terms of gene

presence/absence to estimate gene gain, loss and total substitution rates for both the plasmid and the chromosome compartments. The plasmid gene substitution rate ($1.75x10^{-3}$ gene substitutions per gene and per year 95% HPD: $1.40x10^{-3}$-$2.96x10^{-3}$) appeared to be significantly higher than the chromosome gene substitution rate ($7.00x10^{-5}$, 95% HPD: $6.57x10^{-5}$–$8.21x10^{-5}$). Nevertheless, at the replicon scale, these rates largely overlapped with 0.27 gene substitutions per genome and per year for the plasmid compartment (95% HPD 0.22–0.46) and 0.32 for the chromosomal compartment (95% HPD 0.30–0.38). Chromosome gene gain and loss rates were in the same order of magnitude and showed overlapping 95% HPD (gene gain rate $1.06x10^{-5}$, 95% HPD $7.75x10^{-6}$-$1.55x10^{-5}$ and gene loss rate $5.94x10^{-5}$, 95% HPD $5.70x10^{-5}$-$6.61x10^{-5}$, respectively). The same result was observed for the plasmid compartment (gene gain rate $1.12x10^{-3}$, 95% HPD $9.21x10^{-4}$-$1.68x10^{-3}$ and gene loss rate $6.27x10^{-4}$, 95% HPD $3.98x10^{-4}$-$1.22x10^{-3}$).

A monomorphic and epidemic copper-resistance plasmid

The copper-resistant phenotype was always associated to the presence of pCu^R. Interestingly, the pCu^R gene content was identical for its 42 occurrences (31 in Réunion and 11 in Martinique). We inferred that pCu^R was gained 6.9 times and lost 0.84 times in the phylogeny. Thirty-four filtrated SNPs were detected within pCu^R sequences, but with no significant temporal signal (data not shown). Most of the pCu^R-bearing strains (n=37) formed a monophyletic group within subclade 6, the remaining strains (n=5), originating from Réunion, were distributed in three distinct subclades (Figure 2). The pCu^R SNP diversity was low and identical plasmids (zero SNP) were carried by distantly related strains isolated both in citrus groves and the nursery (Supplementary Figure S4).

Gain, loss and mosaic structure of pathogenicity-related plasmids

In contrast with the dispensable character of pCu^R, all *Xcc* strains known to date encode a pathogenicity-related plasmid gene set, organized as one or multiple plasmids (a few of which have been described (28, 37)). Our short-read and gene-based approach prevented us from reconstructing complete plasmid sequences. However, we were able to assess the presence of the gene content associated to the known *Xcc* plasmid (we used pLH276.2 and pLJ207-7.3 as references (27)) in each strain. This analysis allowed us to define the presence of multiple plasmid alleles (see the right side of Figure 2). Importantly, these alleles were confirmed with long-read sequencing and assembly on a chosen set of strains (strains indicated with an asterisk on Figure 2, Supplementary Table S1). The geographic distribution of the plasmid alleles did not display any clear structure. Indeed, we observed up to six distinct plasmid profiles in a single grove in Réunion.

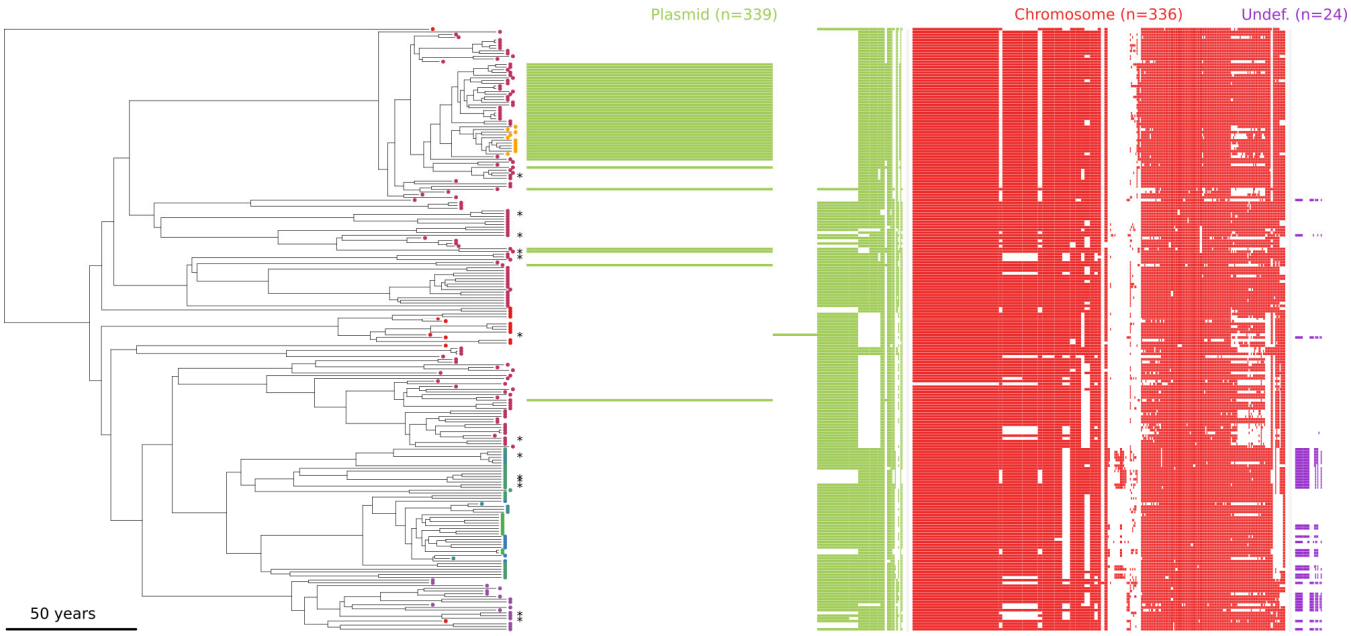

Figure 3. Bayesian phylogeny of the SWIO clade. The matrix on the right of the tree comprises one column for each of the 699 genes that varied in presence/absence among the 221 SWIO strains. A coloured box is printed in front of a strain if it encodes for this gene family. Gene families are separated according to their genetic compartment of origin: plasmid (green), chromosome (red) or undefined (purple). Tips with asterisks indicate strains for which long-read sequencing was also performed.

The plasmid pLH276.2 is a 73kb plasmid closely related to pXac64 (37). In *Xcc*, pXac64-like plasmids typically carry *pthA4*, a transcription activator-like effector (TALE) gene required to produce citrus canker symptoms (22). As expected, a pLH276.2-like plasmid was found in every SWIO strain. Five distinct variations of pLH276.2 were detected. In particular, 49 strains from Mauritius, Réunion and Rodrigues displayed a deletion of 26 genes mostly encoding for plasmid transfer and maintenance functions (Figure 2).

The plasmid pLJ207-7.3 is closely related to pXac47 (38) but comprises a TALE gene whereas pXac47 doesn't. The functions of the proteins encoded by pLJ207-7.3 were mostly unknown (n=24), but included plasmid maintenance and transfer (n=17), as well as other functions (n=15). While most strains from all SWIO islands carried a pLJ207-7.3-like plasmid, it was absent in 77 SWIO strains (Figure 2). Of these, 61 were phylogenetically related and corresponded to all but one individual of clade 6, which included most of the Cu^R strains. Sixteen other strains lacking the plasmid were scattered throughout the phylogeny and had been sampled in Réunion, Mauritius, Mohéli, Mayotte and Rodrigues.

A previously unreported 39.8kb plasmid encoding 40 genes was found in a single strain from Mauritius. The existence of the plasmid was confirmed through long-read sequencing. No other strain presented these genes. Besides conjugation and plasmid partitioning, no specific function could be associated to the plasmid. Similar plasmids (nucleotide identity >75%) were previously found in *Xylella fastidiosa* or *Xanthomonas oryzae* (GenBank accession CP014330.2 and CP007810.1, respectively).

A highly polymorphic chromosomal region

Compared to plasmids, *Xcc* chromosomal gene content was rather homogeneous: we only detected 336 accessory genes. Using gene positions of a high-quality circular chromosome sequence (GenBank accession CP018854.1, from SWIO strain *Xcc* LH276) as a reference, we located 118 SWIO chromosomal accessory genes in one genomic island (GI). The remaining 218 genes were spread along the chromosome in groups of up to seven genes or had no homologue in the chosen reference. The GI did not match recombinant loci, as shown by our analysis and that of Gordon et al. (26). Long-read based *de novo* assemblies of 13 strains demonstrated that the chromosome of *Xcc* is apparently not rearrangement-prone (only one strain displayed a 1.2Mb inversion when compared to LH276 reference chromosome). It also confirmed the extensive variation in the GI's gene content, which carried between 32 and 92 genes, bordered by a phage integrase and a complete IS*3* element on the 5' side and by one or multiple incomplete *AttR* sites on the 3' side. No deviation in GC content was detected for this region (data not shown). In most strains, the GI carried putative multidrug efflux pumps and a class C beta-lactamase was detected in five out of 13 strains. Most notably, the GI comprised one or two usually plasmid-borne TALE genes in seven strains (Figure 4). In addition to the detection of long-reads spanning both the TALE and the adjoining chromosomal region, we were able to produce the expected amplicon by long-template PCR for 4 samples.

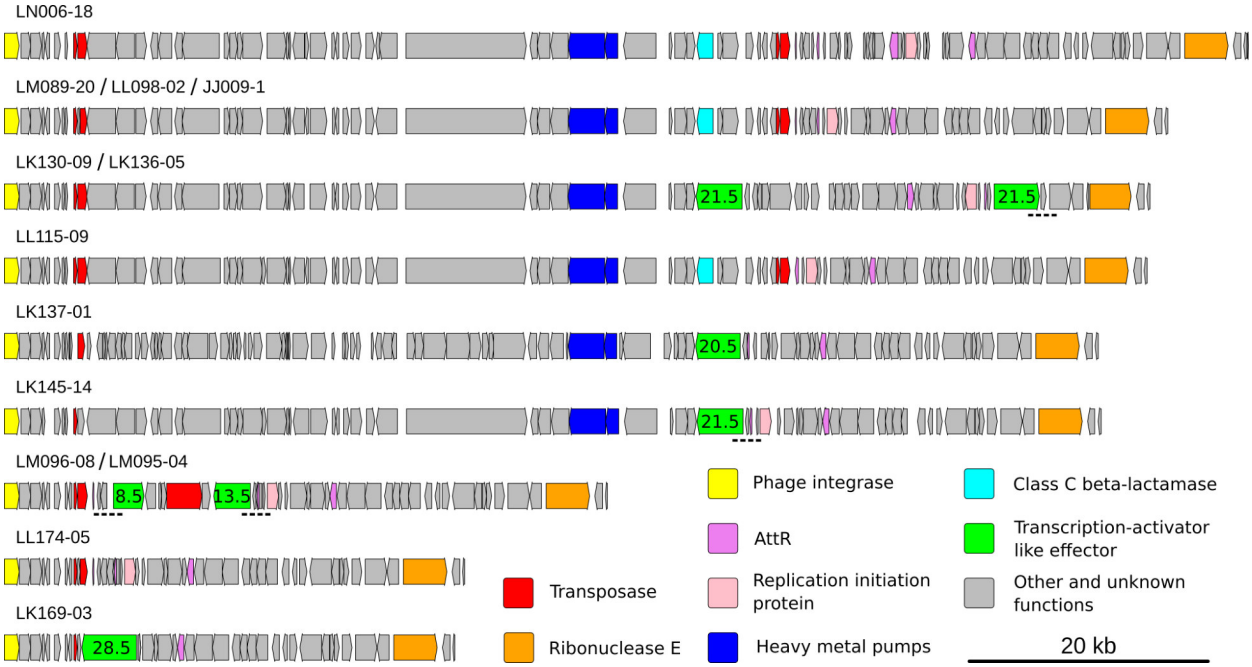

Figure 4. Representation of the gene content of the chromosomal genomic island (corresponding, in LH276, to positions 2 832 588 – 3 003 260) for 13 strains sequenced using long reads. Blocks represent genes homologous to known *Xanthomonas citri* proteins and are coloured according to the predicted function of their encoded proteins (see legend). Number of Repeat Variable Di-residue of Transcription-Activator-Like Effector (TALE) genes, as estimated based on error-prone long reads, are written in the corresponding boxes. Dashed lines highlight regions successfully amplified using long-template PCR. Primers were designed to span both the TALE and the adjoining chromosomal region.

Discussion

In this study, we used a population genomic approach on a monophyletic clade of *Xcc* that causes Asiatic citrus canker outbreaks in the SWIO area. We dated the introduction of *Xcc* in the region to 1762-1868 and were able to reconstruct its local evolutionary history in the SWIO islands. We conjointly inferred the SNP and gene substitution rates and evidenced that gain and loss of accessory genes in *Xcc* is pervasive, even at the most local spatiotemporal scale.

Emergence of *Xcc* in the SWIO area

We used the age of the ancestor of all the strains as a proxy to determine the date when *Xcc* was introduced in the SWIO area. It was estimated to be 1818 (95% HPD: 1762-1868), which predates the earliest report of the disease in the area (1917 in Mauritius, (32)). *Xcc* and its main host genus, *Citrus*, originated in Asia (39, 40) and were probably spread beyond their area of origin by human-mediated movements of plants or plant propagative material. The timeframe suggested here yielded two main hypotheses regarding the origin of the pathogen in the SWIO.

The first hypothesis is that the French botanist and colonial administrator Pierre Poivre (1719-1786) started introducing numerous fruit trees from several Asian countries in the Mascarene Archipelago in the mid-18th century (41) and may have introduced *Citrus* plants infected by *Xcc*. The second hypothesis is that after the abolition of slavery in Mauritius and Réunion in 1835 and 1848, respectively, hundreds of thousands of indentured labourers from several Asian countries (the majority from India) were brought in to boost the agricultural workforce (42-44). This active flow of goods and people from the Asian continent may have led to the concomitant introduction of *Xcc* in the SWIO area. Indeed, the emergence of pre-adapted plant pathogens due to migratory events is a well-recognized phenomenon (45-47). We were unable to accurately identify the geographic origin of the strains that first migrated to the SWIO region. More strains from the hypothetical Asian cradle of *Xcc* will have to be sequenced to provide a definite answer regarding the pathogen's geographic origin and migratory history.

The monophyly of all the SWIO strains contrasts with the genetic diversity found in the northern Indian Ocean and India and indicates that the strains first introduced in the area were closely related, genetically and probably geographically. It also suggests the absence of recent introduction events from remote countries

Genetic structure within SWIO

The SWIO phylogeny displayed a strong geographic structure. However, Réunion and Mauritius strains were both polyphyletic, which meant it was not possible to identify where the first *Xcc* were introduced on the basis of node age. This polyphyly could originate from a polyclonal primary inoculum, a frequent case for *Xcc* (29). It could also evidence ancient exchanges of strains between islands. Indeed, the strain phylogeny also suggests recent inter-island migration events between (i) Mauritius and Rodrigues (a remote Mauritian territory), (ii) the four islands in the Comoros Archipelago and (iii) Réunion and Martinique. In all three cases, political and/or economic links between islands are in accordance with the usual long-range dispersal of *Xcc* through human-associated dispersal of contaminated citrus material (29).

Admixture at citrus grove scale

In contrast with the strong geographic structure of *Xcc* between islands, the analysis of strain diversity obtained after dense sampling in Réunion revealed little concordance between phylogeny and grove location. Strains from a single grove contained up to 300 SNPs, showed variation in terms of gene content (up to 350 genes) and displayed up to six different plasmid gene content profiles. This diverse structure reflects the multiplicity of inoculum inputs that occur during the lifespan of citrus groves. While grove contamination can occur when the grove is first established, it also occurs during periods of wind and rain (*i.e.* storms or hurricanes regularly hit islands in the region) and grove maintenance operations (35). Regardless of their causes these admixture events may be conducive to the horizontal transfer of genes and plasmids and might be crucial for *Xcc* evolution and adaptation.

In Réunion, severe *Xcc* outbreaks occurred during weather conditions which were usually unfavourable to disease development. These were found to be related to the emergence of copper-resistant strains (48). The presence of fully identical pCu^R plasmids in phylogenetically distant strains further confirmed previous data and *in vitro* tests that evidenced this plasmid's mobility. Additionally, the loss rate of pCu^R was found to be seven times lower than its gain rate, suggesting that pCu^R is crucial to *Xcc* in the context of Réunion citriculture with repeated copper applications. Its stability can also reflect the functioning of plasmid maintenance systems such as toxin-antitoxin or partitioning. The gene content uniformity of pCu^R contrasts with its mosaic nature on a broader geographic and phylogenetic scale (27). This suggests that it was recently gained by *Xcc* (30) and has spread rapidly through commercial citrus nurseries.

Chromosome and plasmid mosaicism

While *Xcc* chromosomal synteny and gene content were relatively homogeneous, a region located downstream to a phage integrase and carrying one or multiple partial copies of an *AttR* site in its 3' end was highly variable in terms of gene content and organization. *AttR* and *AttL* motifs result from phage integration into a genome. The lack of the *AttL* motifs within the variable chromosomal region suggests the presence of a non-functional and/or remnant phage.

By activating specific plant genes, bacterial TALE genes are crucial for pathogenicity. Variation in the number and nature of repetitive nucleotide motifs within TALE genes drives the host range of *Xcc* strains (49). Until recently, TALE genes were thought to be only plasmid encoded in *Xcc*. A recent study reported a chromosomal TALE in *Xcc* strains with a restricted host range (known as *Xcc* pathotype A^w) (50). In our study, we report the same result for *Xcc* strains with a broad host range, including all citrus cultivars (pathotype A). Chromosomal TALE genes were carried by a GI of varying size and gene content. In this case, the presence of insertion sequences of the IS*3* family, both in TALE-bearing plasmids and in the GI, may have mediated homologous recombination between plasmid and chromosome, as reported earlier in *Escherichia coli* (51). *Tn3* family transposons have been suggested to have an important role, both in plasmid rearrangement and TALE gene evolution in *Xcc* (28, 52). TnpA, the transposase required for the autonomy of *Tn3* transposons (53) may also have played a role in chromosomal gene acquisition. Indeed, the tripartite element (usually plasmid-encoded) composed of TnpA, bordered by two TALE genes, was found on the chromosome of two strains (Figure 4). Whether these chromosomal TALE genes represent stable integrations or intra-isolate variability remains to be defined and is currently being tested.

In *Xcc* pathotype A, pXac64-like plasmids typically carry a *pthA4* TALE gene. Consistent with the requirement of *pthA4* for disease development (54), we did not find any strains that lacked all pLH276.2 genes or any plasmid-free strains. We evidenced gene content variability of *Xcc* plasmids pLJ207-7.3 and pLH276.2, as shown earlier (28, 55). As suggested by Gochez et al. (28), the location of TALE genes on plasmids and their association with *Tn3* transposons can be highly adaptive. Indeed, *Tn3*-mediated variation in TALE repertoires can provide new alleles. These are shuffled amongst strains via plasmid exchange, which can diffuse adapted combinations. Plasmid plasticity could arise from the acquisition of exogenous genes, as well as from the recombination of existing genetic material. This could be a key feature of *Xcc* evolution.

Rates of evolution: SNP and gene substitution rates

We estimated that the *Xcc* SNP substitution rate comes within the lower range of known bacterial rates (56). While its rate of evolution appeared slow when estimated with standard SNP-based approaches, the gene substitution rate for the *Xcc* SWIO clade was three orders of magnitude higher than SNP mutation rates when expressed on a per-site basis. Previous studies involving similar analyses reported that gene turnover rates were in the same order of magnitude as the SNP rate (15-18). It is important to note that these studies were performed at deeper phylogenetic scales than ours. Indeed, the gene substitution rate is highly dependent on the evolutionary timescale considered, given that most gene content variations are short lived (13, 19, 57). Assuming that most gene content variations were deleterious, Vos et al. (19) suggested that the ratio of gene content changes to mutation is likely to be very high for closely related genomes. Our results clearly confirm their supposition. Whether such a high gene turnover is being selected because it secures the access to rare but beneficial accessory genes remains debated (19, 58). Chromosome and plasmid gene substitutions per gene and per year were 7.00×10^{-5} and 1.75×10^{-3}, respectively. Importantly, the genuine gene substitution rate may be different from the one we observed because the evolutionary history of horizontally transferred DNA may differ from that of the bacterial host. Here, we intend to determine the gene turnover rate of the bacterial host.

We observed high heterogeneity in gene turnover rates between subclades, which probably reflects the fact that numerous genes are gained simultaneously through plasmid integration. In the SWIO lineage, pCu^R is a good example of a recently acquired and successfully maintained mobile genetic element. However, the future trajectory of pXac39, a previously uncharacterized plasmid observed in a single strain, remains unknown and will depend on how it affects host fitness. Plasmids appeared much more permeable to exogenous genetic material than chromosomes, with a gene turnover rate three orders of magnitude higher. Therefore, plasmids represent a privileged type of vehicle for accessory genes in *Xcc*, which is consistent with earlier network analyses (8).

Concluding remarks

In this study, we reconstructed the genomic evolution of a lineage of the citrus pathogenic bacterium *Xcc* from its emergence in SWIO in the 19th century to its global endemicity with epidemic waves nowadays. This lineage displayed a low SNP substitution rate, characteristic of monomorphic bacterium. In contrast to this apparently slow rate of evolution, we revealed the cardinal importance of genomic evolution through gene gain and loss. The plasmid compartment played a key role in gene-based evolution: a drug-resistance plasmid spread among the SWIO lineage and pathogenicity-related plasmids exhibited extensive plasticity. By favouring intra-cellular recombination, *Tn3* transposons and IS*3* elements might play an important role in genomic plasticity. Lastly, by describing chromosomal TALE genes for the first time in broad host range *Xcc* strains, our study also opens up a new line of investigation in the field of host/pathogen interaction.

Materials and Methods

DNA extraction and sequencing of bacterial strains

The dataset comprised whole genome sequences for 284 *Xcc* strains, including 210 strains from the South West Indian Ocean (SWIO; Figure 1, Supplementary Table S2). All the strains were sequenced using Illumina. Long-read Oxford Nanopore MinION sequencing was also performed on 13 selected strains. Copper-resistance phenotypes were determined previously (30). DNA sequencing and data processing are detailed in (59).

SNP detection

We used a custom bioinformatics pipeline to obtain a filtered set of SNPs from the Illumina raw reads (Supplementary Figure S5). In short, after a quality control trimming step using Trimmomatic v. 0.36 (60), reads were aligned against the chromosome of *Xcc* strain IAPAR 306 (GenBank accession NC_003919.1) with BWA-MEM v. 0.7.15 (61). *Xcc* strains displayed a mean coverage of 232 (Table S2). Duplicated reads were removed using PicardTools MarkDuplicates v. 2.7. Indel realignment and SNP calling were performed using Freebayes 0.9.21-5 (62). SNPs were then filtered based on allele number, coverage, phred quality, allele frequency or genomic characteristics, such as SNP density or repeated genomic regions. In order to exclude SNPs found in regions that had undergone homologous recombination from the follow-up phylogenetic analyses, we searched for recombinant regions with ClonalFrameML (63) and RDP4 (64) using default parameters. Recombination analysis using ClonalframeML detected a 136kb recombinant region, comprising 233 SNPs in seven strains originating from Mali, Senegal, Bangladesh and India. The RDP4 analysis detected a 197kb (315 SNPs) recombinant region entirely overlapping the region detected with ClonalFrameML. These 315 SNPs were thus excluded from the global dataset for subsequent phylogenetic reconstruction and molecular clock analysis.

We first tested the adequacy of several models of molecular evolution with our SNP set. According to PartitionFinder v.2.1.1 and based on Bayesian Information Criterion, the model of evolution best fitting our dataset was a General Time-Reversible substitution model of evolution with variation among sites modelled with a discrete Gamma distribution and Invariant sites (GTR+G+I) (65). We reconstructed a Maximum Likelihood tree of the global dataset using RAxML v.8.2.9 (66). The presence of the temporal signal in the dataset was tested by computing the linear regression between sample age and root-to-tip distances at every internal node of the Maximum Likelihood tree (67). The SWIO clade root was the deepest node for which both the linear regression was statistically significant and the slope positive. The

SWIO clade was, therefore, assumed to contain detectable amounts of evolutionary change, making it suitable for tip-dating inferences. A date-randomization test with 20 replicates was performed to confirm the presence of the temporal signal (68).

Tip-dating inference was then performed on the SWIO subset using BEAST v1.8.4 (36) with a GTR+G+I substitution model of evolution. We used an uncorrelated lognormal relaxed clock to account for rate variation among lineages. To minimize prior assumptions about demographic history, we first used an extended Bayesian skyline plot to integrate data over different coalescent histories. After inspecting the demographic reconstruction, an exponential growth was established as a best fit for the tree prior. Three independent chains were run for 100 000 000 steps and sampled every 10 000 steps. The first 1 000 samples (10%) were discarded as burn-in. Convergence to the stationary distribution and sufficient sampling and mixing were checked by inspecting posterior samples using Tracer v1.6 (effective sample size >200) (69). After combining the three runs, a maximum clade credibility tree was obtained with TreeAnnotator v1.10.2 (36).

Core and accessory genome assignation

Our estimation of the gene content of each strain from the SWIO clade relied on a two-step approach. We first estimated the total SWIO homologous set of genes with a pipeline combining *de novo* assembly, gene prediction and gene clustering (Supplementary Figure S6). We then defined the gene content of individual strains. To validate our gene content analysis method, we first analysed three sequenced replicates of two strains (*Xcc* LH201 and *Xcc* LE50), both already sequenced using the long-read Pacific Biosciences RSII technology (Supplementary Figure S6). Besides assessing the error rate associated with our pipeline, the replicates were used to tune the mapping parameters that were to consider a gene present in a strain. Importantly, distinct bacterial cultures and DNA extractions were performed for each of the replicates. Therefore, our estimate will confound the genuine variation resulting from gene loss during culture and the variation associated with the bioinformatics pipeline. Lastly, we mapped each strain's reads on the set of 5 046 homologous genes (Supplementary Table S2). We defined the gene content of individual strains using the parameters minimizing gene content variations between replicates (a gene was considered present in a strain if coverage was ≥20x over at least 60% of its length).

Genomic location of gene clusters to the chromosome or plasmids was informed by the available circularized Pacific Biosciences-sequenced reference genomes. Genomic location of unassigned gene clusters was defined based on the location of genes co-occurring on the same contigs. Functions were

assigned to the gene clusters according to their amino-acid homology (using a 30% identity/30% length threshold) with known Clusters of Orthologous Groups (COGs) based on a BLASTx search.

In a second BEAST analysis using the previously inferred tree topology, a discrete model was used to reconstruct the ancestral states of gene presence/absence. Three independent chains were run as described above. Mean and 95% HPD gene substitution rate, gain rate and loss rate were obtained from the parameter distribution using a custom Perl script and the R HDInterval package (70). Rates of gene gain and loss were defined as the number of state changes (present or absent) per site per year, using the mean number of plasmid-borne and chromosomal genes per strain as the site number.

With the exception of the thirteen Minion-sequenced strains (Supplementary Table S1), the nature of our sequencing data prevented us from assembling closed, circularized plasmid genomes. However, using each strain's gene content, we could assess each strain for the presence of genes previously identified on closed plasmids. High quality PacBio-based circular plasmid sequences were used as the genomic reference for each plasmid's gene content and synteny: pLJ207-7.3 (GenBank accession CP018853.1, from SWIO strain *Xcc* LJ207-7, related to pXac47 (38)), pLH276.2 (GenBank accession CP018856.1, from SWIO strain *Xcc* LH276, related to pXac64 (37)), and the copper-resistance plasmid pCu^R (GenBank accession CP018859, from SWIO strain *Xcc* LH201 (27)).

Data availability

The sequencing data generated in this study have been published in the NCBI GenBank repository under accession numbers listed in Supplementary Table S2, Additional File 1.

Acknowledgements

We would like to express our thanks to the Plant Protection Platform (3P, IBISA) and to S. Javegny, K. Boyer and J. Hascoat for their helpful contribution. The European Regional Development Fund (ERDF contract GURDT I2016-1731-0006632), the Réunion Region, the French government, the French Agropolis Foundation (Labex Agro – Montpellier, E-SPACE project number 1504-004), ANSES and CIRAD provided financial support. We would like to thank INRAPE (the Union of the Comoros), FAREI (Mauritius) and NBA (Seychelles) for providing us with diseased citrus material. This work was supported by the CIRAD - UMR AGAP HPC Data Center of the South Green Bioinformatics platform (http://www.southgreen.fr/).

Funding

The European Regional Development Fund (ERDF contract GURDT I2016-1731-0006632), the Réunion Region, the French government, the French Agropolis Foundation (Labex Agro – Montpellier, E-SPACE project number 1504-004), ANSES and CIRAD provided financial support.

Author contributions

D.R., O.P. and P.L. designed and conceived the study; C.B. processed the samples in the wet-lab; D.R. performed computational analyses with inputs from P.L. and A.R.; D.R., P.L. and O.P. wrote the manuscript with inputs from all co-authors.

References

1. Croucher NJ, Harris SR, Grad YH, Hanage WP. 2013. Bacterial genomes in epidemiology-present and future. Philosophical Transactions of the Royal Society B: Biological Sciences 368:20120202.
2. Estoup A, Guillemaud T. 2010. Reconstructing routes of invasion using genetic data: why, how and so what? Molecular ecology 19:4113-4130.
3. Ruh M, Briand M, Bonneau S, Jacques M-A, Chen NW. 2017. *Xanthomonas* adaptation to common bean is associated with horizontal transfers of genes encoding TAL effectors. BMC genomics 18:670.
4. Monteil CL, Yahara K, Studholme DJ, Mageiros L, Meric G, Swingle B, Morris CE, Vinatzer BA, Sheppard SK. 2016. Population-genomic insights into emergence, crop adaptation and dissemination of *Pseudomonas syringae* pathogens. Microbial Genomics 2:e000089.
5. Chen NW, Serres-Giardi L, Ruh M, Briand M, Bonneau S, Darrasse A, Barbe V, Gagnevin L, Koebnik R, Jacques M-A. 2018. Horizontal gene transfer plays a major role in the pathological convergence of *Xanthomonas* lineages on common bean. BMC genomics 19:606.
6. Vinatzer BA, Monteil CL, Clarke CR. 2014. Harnessing population genomics to understand how bacterial pathogens emerge, adapt to crop hosts, and disseminate. Annual review of phytopathology 52:19-43.
7. Achtman M. 2012. Insights from genomic comparisons of genetically monomorphic bacterial pathogens. Philosophical Transactions of the Royal Society B: Biological Sciences 367:860-7.
8. Halary S, Leigh JW, Cheaib B, Lopez P, Bapteste E. 2010. Network analyses structure genetic diversity in independent genetic worlds. Proceedings of the National Academy of Sciences, USA 107:127-32.
9. Osborn AM, Böltner D. 2002. When phage, plasmids, and transposons collide: genomic islands, and conjugative-and mobilizable-transposons as a mosaic continuum. Plasmid 48:202-212.

10. Hall JPJ, Brockhurst MA, Harrison E. 2017. Sampling the mobile gene pool: innovation via horizontal gene transfer in bacteria. Philosophical Transactions of the Royal Society B: Biological Sciences 372:20160424.

11. Didelot X, Maiden MCJ. 2010. Impact of recombination on bacterial evolution. Trends in Microbiology 18:315-322.

12. Darmon E, Leach DR. 2014. Bacterial genome instability. Microbiology and Molecular Biology Reviews 78:1-39.

13. Gogarten JP, Townsend JP. 2005. Horizontal gene transfer, genome innovation and evolution. Nature Reviews Microbiology 3:679-87.

14. Ochman H, Lawrence JG, Groisman EA. 2000. Lateral gene transfer and the nature of bacterial innovation. Nature 405:299-304.

15. Touchon M, Hoede C, Tenaillon O, Barbe V, Baeriswyl S, Bidet P, Bingen E, Bonacorsi S, Bouchier C, Bouvet O. 2009. Organised genome dynamics in the *Escherichia coli* species results in highly diverse adaptive paths. PLoS genetics 5:e1000344.

16. Marri PR, Hao W, Golding GB. 2006. Gene gain and gene loss in *Streptococcus*: is it driven by habitat? Molecular biology and evolution 23:2379-2391.

17. Marri PR, Hao W, Golding GB. 2007. The role of laterally transferred genes in adaptive evolution. BMC evolutionary biology 7:S8.

18. Hao W, Golding GB. 2006. The fate of laterally transferred genes: life in the fast lane to adaptation or death. Genome research 16:636-643.

19. Vos M, Hesselman MC, te Beek TA, van Passel MW, Eyre-Walker A. 2015. Rates of lateral gene transfer in prokaryotes: high but why? Trends in microbiology 23:598-605.

20. McManus PS, Stockwell VO, Sundin GW, Jones AL. 2002. Antibiotic use in plant agriculture. Annual review of phytopathology 40:443-465.

21. Thynne E, McDonald MC, Solomon PS. 2015. Phytopathogen emergence in the genomics era. Trends in Plant Science 20:246-255.

22. Swarup S, De Feyter R, Brlansky RH, Gabriel DW. 1991. A pathogenicity locus from *Xanthomonas citri* enables strains from several pathovars of *X. campestris* to elicit cankerlike lesions on citrus. Phytopathology 81:802-809.

23. Barash I, Manulis-Sasson S. 2009. Recent evolution of bacterial pathogens: the gall-forming *Pantoea agglomerans* case. Annual review of phytopathology 47:133-152.

24. Pilla G, Tang CM. 2018. Going around in circles: virulence plasmids in enteric pathogens. Nature Reviews Microbiology 16:484-95.

25. Kado CI. 2015. Historical events that spawned the field of plasmid biology, p 3-11, Plasmids: Biology and Impact in Biotechnology and Discovery. American Society of Microbiology.

26. Gordon JL, Lefeuvre P, Escalon A, Barbe V, Cruveiller S, Gagnevin L, Pruvost O. 2015. Comparative genomics of 43 strains of *Xanthomonas citri* pv. *citri* reveals the evolutionary events giving rise to pathotypes with different host ranges. BMC Genomics 16:1098.

27. Richard D, Ravigne V, Rieux A, Facon B, Boyer C, Boyer K, Grygiel P, Javegny S, Terville M, Canteros BI, Robene I, Verniere C, Chabirand A, Pruvost O, Lefeuvre P. 2017. Adaptation of genetically monomorphic bacteria: evolution of copper resistance through multiple horizontal gene transfers of complex and versatile mobile genetic elements. Molecular Ecology 26:2131-2149.

28. Gochez AM, Huguet-Tapia JC, Minsavage GV, Shantaraj D, Jalan N, Strauss A, Lahaye T, Wang N, Canteros BI, Jones JB, Potnis N. 2018. Pacbio sequencing of copper-tolerant *Xanthomonas citri* reveals presence of a chimeric plasmid structure and provides insights into reassortment and shuffling of transcription activator-like effectors among *X. citri* strains. BMC Genomics 19:16.

29. Leduc A, Traore YN, Boyer K, Magne M, Grygiel P, Juhasz CC, Boyer C, Guerin F, Wonni I, Ouedraogo L, Verniere C, Ravigne V, Pruvost O. 2015. Bridgehead invasion of a monomorphic plant pathogenic bacterium: *Xanthomonas citri* pv. *citri*, an emerging citrus pathogen in Mali and Burkina Faso. Environmental Microbiology 17:4429-42.

30. Richard D, Tribot N, Boyer C, Terville M, Boyer K, Javegny S, Roux-Cuvelier M, Pruvost O, Moreau A, Chabirand A, Vernière C. 2017. First report of copper-resistant *Xanthomonas citri* pv. *citri* pathotype A causing asiatic citrus canker in Réunion, France. Plant Disease 100:1946.

31. Wiehe PO. 1941. Report on plant pathologist's visit to Rodrigues. Ministry of Agriculture, Fisheries and Food:16.

32. Aubert B. 2014. Vergers de la Réunion et de l'Océan Indien, CIRAD, Montpellier, France ed.

33. Brun J. 1971. Le chancre bactérien des *Citrus*. Fruits 26:533-540.

34. Bradbury JF. 1986. Guide to plant pathogenic bacteria. CABI, Slough, UK.

35. Graham JH, Gottwald TR, Cubero J, Achor DS. 2004. *Xanthomonas axonopodis* pv. *citri*: factors affecting successful eradication of citrus canker. Molecular Plant Pathology 5:1-15.

36. Drummond AJ, Rambaut A. 2007. BEAST: bayesian evolutionary analysis by sampling trees. BMC evolutionary biology 7:214.

37. Da Silva AC, Ferro JA, Reinach FC, Farah CS, Furlan LR, Quaggio RB, Monteiro-Vitorello CB, Van Sluys MA, Almeida NF, Alves LM, do Amaral AM, Bertolini MC, Camargo LE, Camarotte G, Cannavan F, Cardozo J, Chambergo F, Ciapina LP, Cicarelli RM, Coutinho LL, Cursino-Santos JR, El-Dorry H, Faria JB, Ferreira AJ, Ferreira RC, Ferro MI, Formighieri EF, Franco MC, Greggio CC, Gruber A, Katsuyama AM, Kishi LT, Leite RP, Lemos EG, Lemos MV, Locali EC, Machado MA, Madeira AM, Martinez-Rossi NM, Martins EC, Meidanis J, Menck CF, Miyaki CY, Moon DH, Moreira LM, Novo MT, Okura VK, Oliveira MC, Oliveira VR, Pereira HA, et al. 2002. Comparison of

the genomes of two *Xanthomonas* pathogens with differing host specificities. Nature 417:459-63.

38. Martins PMM, Machado MA, Silva NV, Takita MA, de Souza AA. 2016. Type II toxin-antitoxin distribution and adaptive aspects on *Xanthomonas* genomes: focus on *Xanthomonas citri*. Frontiers in microbiology 7:652-652.

39. Pruvost O, Magne M, Boyer K, Leduc A, Tourterel C, Drevet C, Ravigne V, Gagnevin L, Guerin F, Chiroleu F, Koebnik R, Verdier V, Verniere C. 2014. A MLVA genotyping scheme for global surveillance of the citrus pathogen *Xanthomonas citri* pv. *citri* suggests a worldwide geographical expansion of a single genetic lineage. PLoS One 9:e98129.

40. Wu GA, Terol J, Ibanez V, López-García A, Pérez-Román E, Borredá C, Domingo C, Tadeo FR, Carbonell-Caballero J, Alonso R, Curk F, Du D, Ollitrault P, Roose ML, Dopazo J, Gmitter FG, Rokhsar DS, Talon M. 2018. Genomics of the origin and evolution of *Citrus*. Nature 554:311.

41. Du Pont de Nemours PS. 1797. Oeuvres complètes de P. Poivre, intendant des isles de France et de Bourbon, correspondant de l'académie des sciences, etc., Fuchs eds., Paris, France ed.

42. Carter MT, K. 2002. Coolitude: an anthology of the Indian labour diaspora, London, UK: Anthem Press. ed.

43. Campbell PC. 1923. Chinese coolie emigration to countries within the British empire, Westminster, UK: King & Son. ed.

44. Govindin SS. 1994. Les engagés indiens: Ile de la Réunion, XIXe siècle, Saint Denis, France: Azalées Éditions ed.

45. Anderson PK, Cunningham AA, Patel NG, Morales FJ, Epstein PR, Daszak P. 2004. Emerging infectious diseases of plants: pathogen pollution, climate change and agrotechnology drivers. Trends in Ecology & Evolution 19:535-544.

46. Yoshida K, Schuenemann VJ, Cano LM, Pais M, Mishra B, Sharma R, Lanz C, Martin FN, Kamoun S, Krause J. 2013. The rise and fall of the *Phytophthora infestans* lineage that triggered the Irish potato famine. Elife 2:e00731.

47. McDonald BA, Stukenbrock EH. 2016. Rapid emergence of pathogens in agro-ecosystems: global threats to agricultural sustainability and food security. Philosophical Transactions of the Royal Society B: Biological Sciences 371:20160026.

48. Pruvost O, Boyer K, Ravigné V, Richard D, Vernière C. 2019. Deciphering how plant pathogenic bacteria disperse and meet: Molecular epidemiology of *Xanthomonas citri* pv. *citri* at microgeographic scales in a tropical area of Asiatic citrus canker endemicity. Evolutionary Applications 12:1523-38.

49. Ference CM, Gochez AM, Behlau F, Wang N, Graham JH, Jones JB. 2018. Recent advances in the understanding of *Xanthomonas citri* ssp. *citri* pathogenesis and citrus canker disease management. Molecular plant pathology 19:1302-1318.

50. Munoz Bodnar A, Santillana G, Mavrodieva V, Liu Z, Nakhla M, Gabriel DW. 2017. Complete genome sequences of three *Xanthomonas citri s*trains from Texas. Genome Announcements 5:e00609-17.

51. Deonier RC, Hadley R. 1980. IS*2*-IS*2* and IS*3*-IS*3* relative recombination frequencies in F integration. Plasmid 3:48-64.

52. Ferreira RM, de Oliveira AC, Moreira LM, Belasque J, Jr., Gourbeyre E, Siguier P, Ferro MI, Ferro JA, Chandler M, Varani AM. 2015. A TALE of transposition: Tn*3*-like transposons play a major role in the spread of pathogenicity determinants of *Xanthomonas citri* and other xanthomonads. MBio 6:e02505-14.

53. Nicolas E, Lambin M, Dandoy D, Galloy C, Nguyen N, Oger CA, Hallet B. 2015. The Tn*3*-family of replicative transposons. Microbiology Spectrum 3:MDNA3-0060-2014.

54. Brunings AM, Gabriel DW. 2003. *Xanthomonas citri*: breaking the surface. Molecular Plant Pathology 4:141-57.

55. Carvalho FMdS, Caramori LPC, Leite Júnior RP. 2005. Genetic diversity of *Xanthomonas axonopodis* pv. *citri* based on plasmid profile and pulsed field gel electrophoresis. Genetics and Molecular Biology 28:446-451.

56. Duchene S, Holt KE, Weill FX, Le Hello S, Hawkey J, Edwards DJ, Fourment M, Holmes EC. 2016. Genome-scale rates of evolutionary change in bacteria. Microbial Genomics 2:e000094.

57. Nowell RW, Green S, Laue BE, Sharp PM. 2014. The extent of genome flux and its role in the differentiation of bacterial lineages. Genome biology and evolution 6:1514-1529.

58. Bolotin E, Hershberg R. 2017. Horizontally acquired genes are often shared between closely related bacterial species. Frontiers in microbiology 8:1536.

59. Richard D, Pruvost O. 2020. Complete genome sequences of 284 *Xanthomonas citri* pv. *citri* strains causing Asiatic citrus canker. Microbiology Resource Announcements (in press).

60. Bolger AM, Lohse M, Usadel B. 2014. Trimmomatic: a flexible trimmer for Illumina sequence data. Bioinformatics 30:2114-2120.

61. Li H. 2013. Aligning sequence reads, clone sequences and assembly contigs with BWA-MEM. arXiv preprint arXiv:13033997.

62. Garrison E, Marth G. 2012. Haplotype-based variant detection from short-read sequencing. arXiv preprint arXiv:12073907.

63. Didelot X, Wilson DJ. 2015. ClonalFrameML: efficient inference of recombination in whole bacterial genomes. PLoS computational biology 11:e1004041.

64. Martin DP, Murrell B, Golden M, Khoosal A, Muhire B. 2015. RDP4: detection and analysis of recombination patterns in virus genomes. Virus evolution 1:vev003.

65. Lanfear R, Frandsen PB, Wright AM, Senfeld T, Calcott B. 2016. PartitionFinder 2: new methods for selecting partitioned models of evolution for molecular and morphological phylogenetic analyses. Molecular Biology and Evolution 34:772-773.

66. Kozlov A, Darriba D, Flouri T, Morel B, Stamatakis A. 2019. RAxML-NG: A fast, scalable, and user-friendly tool for maximum likelihood phylogenetic inference. Bioinformatics 35:4453-5.

67. Jombart T, Balloux F, Dray S. 2010. adephylo: new tools for investigating the phylogenetic signal in biological traits. Bioinformatics 26:1907-9.

68. Duchene S, Duchene D, Holmes EC, Ho SY. 2015. The performance of the date-randomization test in phylogenetic analyses of time-structured virus data. Molecular Biology and Evolution 32:1895-906.

69. Rambaut A, Suchard M, Xie D, Drummond A. 2014. Tracer, version 1.6, MCMC trace analysis package [Internet].

70. Meredith M, Kruschke J. 2016. HDInterval: highest (posterior) density intervals. R package version 01 3.